

MAGNETOHYDRODYNAMIC FREE CONVECTION HEAT TRANSFER FROM AN EXPONENTIALLY STRETCHING SURFACE IN A NON-DARCIAN SATURATED POROUS MEDIUM

M. SUBHAS ABEL, VEENAM.BASANGOUDA

Abstract: We examine the effects of porous impedance on laminar magnetohydrodynamic free convection heat transfer of an electrically-conducting, Newtonian, Boussinesq fluid from a vertical stretching surface in a non-Darcian porous medium under the influence of uniform transverse magnetic field. The flow is considered over a stretching sheet in the presence of viscous dissipation and internal heat generation. The well-known Boussinesq approximation has been used to represent the buoyancy term adding to the governing equation. By applying two equal and opposing forces along the x -axis, the sheet is stretched with a speed proportional to the distance from the fixed origin $x = 0$. Similarity transformations are used to reduce the governing boundary layer equations to coupled higher order non-linear ordinary differential equations. These equations were numerically solved using implicit finite difference scheme known as Keller box method. The computed results are compared with the previously reported work and have good agreement with earlier studies. The effects of various physical parameters like Porous parameter, Prandtl number, Hartmann number, Grashoff number, inertia coefficient, and internal heat generation on flow, and heat transfer characteristics are reported graphically in detail. Applications of the study include magnetic materials processing and chemical engineering systems.

Keywords: Non-Darcian saturated porous medium, Keller box method, Prandtl number, free convection, MHD

Introduction: Aerodynamic extrusion of plastic sheets, glass fiber production, paper production, heat treated materials travelling between a feed roll and a wind-up roll, cooling of an infinite metallic plate in a cooling bath, manufacturing of polymeric sheets are some examples for practical applications of boundary layer fluid flow over a stretching surface. For the production of fiber sheet/plastic sheet, extrusion of molten polymers through a slit die is an important process in polymer industry. This thermo-fluid problem involves significant heat transfer between the sheet and the surrounding fluid. In this process the extrudate starts to solidify as soon as it exits from the die and then the sheet is collected by a wind-up roll upon solidification. The quality of the final product depends on the rate of heat transfer and the stretching rate. This stretching may not necessarily be linear. It may be quadratic, power-law, exponential and so on. The inertia effect is assumed to be important at higher flow rate and it can be accounted for through the addition of a velocity-squared term in the momentum equation, which is known as the Forchheimer extension. The Brinkman extension is usually used to shed light on the importance of boundary effects. Especially in heat transfer problems the variation of density with temperature give rise to a buoyancy force under natural convection.

After the pioneering work of Sakiadis (1961a, 1961b), many researchers gave attention to study flow and heat transfer of Newtonian and non-Newtonian fluids over a linear stretching sheet. By considering

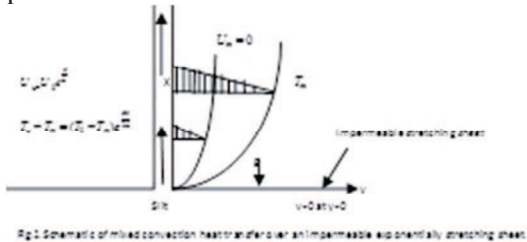
quadratic stretching sheet, Kumaran and Ramanaiah (1996) analyzed the problem of heat transfer. Ali (1995) investigated the thermal boundary layer flow on a power law stretching surface with suction or injection.

Elbashbeshy (2001) analyzed the problem of heat transfer over an exponentially stretching sheet with suction. Magyari and Keller (1999) discussed the heat and mass transfer in boundary layers on an exponentially stretching continuous surface. Khan and Sanjayanand (2005) and Sanjayanand and Khan (2006) extended the work of Elbashbeshy (2001) to viscoelastic fluid flow, heat and mass transfer over an exponentially stretching sheet. Raptis et al. (1981) constructed similarity solutions for boundary layer near a vertical surface in a porous medium with constant temperature and concentration. Bejan and Khair (1985) used Darcy's law to study the features of natural convection boundary layer flow driven by temperature and concentration gradients.

Forchheimer (1901) proposed quadratic term in Darcian velocity to describe the inertia effect in a porous medium. Plumb and Huenefeld (1981) studied the problem of non-Darcian free convection over a vertical isothermal flat plate. Rees and Pop (1994) also studied the free convection flow along a vertical wavy surface with constant wall temperature. Rees and Pop (1995) studied the case where the heated surface displays waves while the Darcy law is supplemented by the Forchheimer terms. They stated that the boundary flow remains self similar in the presence of

surface waves where the inertia is absent, and when the inertia is present the surface waves are absent. However, the combination of the two effects yields non-similarity. Tsou et al. (1967) studied flow and heat transfer in the boundary layer on a continuous moving surface, while Gupta and Gupta (1977) solved boundary layer flow with suction and injection. Andersson and Bech (1992) have studied the MHD flow of the power law fluid over stretching sheet. Pavlov (1974) gave an exact similarity solution to the MHD boundary layer equation for the steady and two dimensional flow caused solely by the stretching of an elastic surface in the presence of uniform magnetic field. Abel and Mahesha (2008)

Motivated by the above-mentioned studies, it is noticed that the effect of non-Darcian boundary layer flow was not studied so far for exponentially stretching sheet. Therefore, this paper can be used as a bridge to fill the knowledge gap. It is an extension of the work of Pal (2010) through the introduction of an additional parameter, i.e., the drag coefficient parameter. This study has applications in the effect of solid boundary and inertial forces on flow and heat transfer in porous media. The governing boundary-value problem has been numerically solved using an implicit finite difference scheme known as the Keller box method. From the above-cited literature, we can realize that the Keller box method has not been widely used. The results obtained from the present investigation will provide useful information for application and also serve as a complement to the previous studies.



Mathematical Formulation: Consider a steady laminar two dimensional boundary layer flow and heat transfer over an exponentially stretching sheet in an electrically conducting quiescent fluid coinciding with the plane $y = 0$, the flow being confined to exponential temperature distribution T_w are defined as follows:

$$U_w(x) = U_0 e^{\frac{x}{L}}, \quad \text{"(6)",} \quad (6)$$

$$T_w(x) = T_\infty + (T_0 - T_\infty) e^{\frac{ax}{2L}}, \quad \text{"(7)",} \quad (7)$$

where T_0 and a are parameters of temperature distribution over the stretching surface.

Further, we look for a similarity transformation of equations (1) to (3) by introducing the following similarity transformation:

$y > 0$. The x -axis runs along the stretching sheet and y -axis perpendicular to it. A uniform magnetic field of strength B_0 is assumed to be applied in the y -direction. It is assumed that the induced magnetic field of the flow is negligible in comparison with the applied one which corresponds to a very small magnetic Reynolds number. The continuity, momentum and energy equations can be written as

$$\frac{\partial u}{\partial x} + \frac{\partial v}{\partial y} = 0 \quad \text{"(1)",} \quad (1)$$

$$u \frac{\partial u}{\partial x} + v \frac{\partial u}{\partial y} = \nu \frac{\partial^2 u}{\partial y^2} - \frac{\nu}{k} u - \frac{C_b}{\sqrt{k}} u^2 + g\beta(T - T_\infty) - \sigma \frac{B_0^2}{\rho} u \quad \text{"(2)",} \quad (2)$$

$$u \frac{\partial T}{\partial x} + v \frac{\partial T}{\partial y} = \alpha \frac{\partial^2 T}{\partial y^2} + \frac{\sigma}{\rho C_p} B_0^2 u^2 + \frac{\mu}{\rho C_p} \left(\frac{\partial T}{\partial y} \right)^2 + \frac{Q}{\rho C_p} (T - T_\infty) \quad \text{"(3)",} \quad (3)$$

The associated boundary conditions to the problem are

$$U = U_w(x), \quad v = 0, \quad T = T_w(x) \text{ at } y = 0, \quad \text{"(4)",} \quad (4)$$

$$u = 0, \quad T \rightarrow T_\infty \text{ as } y \rightarrow \infty, \quad \text{"(5)",} \quad (5)$$

where u and v are the x and y components of the velocity field of the steady plane boundary flow, respectively, ν denotes the kinematic viscosity, k is the permeability of the porous medium, α is the thermal diffusivity of the ambient fluid, σ is the electrical conductivity, and B_0 is the magnetic field flux density. The fluid flow is under the effect of the temperature field, where T_∞ is the temperature of the ambient fluid, Q is internal heat generation/absorption coefficient, and C_b is the drag coefficient. The stretching velocity U_w and

$$\eta = \sqrt{\frac{\text{Re} y}{2L}} e^{\frac{x}{2L}}, \quad \psi(x, \eta) = \sqrt{2 \text{Re} \nu} e^{2L} f(\eta), \quad \text{"(8)", (8)}$$

$$T(x, y) = T_\infty + (T_0 - T_\infty) e^{2L} \theta(\eta), \quad \text{"(9)", (9)}$$

where ψ is the stream function which is defined in the usual form as

$$u = \frac{\partial \psi}{\partial y} \text{ and } v = -\frac{\partial \psi}{\partial x} \quad \text{"(10)", (10)}$$

Thus substituting Eqs.(8) and (9) into Eq. (10), we obtain u and v as follows:

$$u(x, y) = u_0 e^{\frac{x}{L}} f'(\eta), \quad \text{"(11)",}$$

$$v(x, y) = -\frac{\nu}{L} \sqrt{\frac{\text{Re}}{2}} e^{2L} [f(\eta) + \eta f'(\eta)]. \quad \text{"(12)",}$$

Equations (1)-(5) are transformed into nonlinear ordinary differential equations, with the aid of Eqs. (8)-(12). Thus, the governing equations takes the form

$$f''' + ff'' - (2 + N_2) f'^2 + 2 \text{Gre}^{\frac{\alpha x}{2}} e^{-2x} \theta - 2e^{-x} f' \left(\frac{\text{Ha}^2}{\text{Re}} + N_1 \right) = 0 \quad \text{"(13)", (12)}$$

$$\text{Pr}^{-1} \theta'' + f \theta' - a f' \theta + e^{\frac{X(2-a)}{2}} \text{Ec} \left(2 \frac{\text{Ha}^2}{\text{Re}} f'^2 + f''^2 e^X \right) + 2 \lambda e^{-X} \theta = 0 \quad \text{"(14)",}$$

(13)

Further the boundary conditions, Eqs. (4) and (5) reduces to the form,

$$C_f \sqrt{\text{Re}_x} = \sqrt{2X} f''(0), \quad f(0) = 0, \quad \text{"(14)}$$

$$f'(0) = 1, \quad \theta(0) = 1,$$

$$f'(\infty) = 0, \quad \theta(\infty) = 0, \quad \text{"(15)}$$

where $X = x / L$, $\text{Ha} = (\sigma B_0^2 L^2 / \rho \nu)^{\frac{1}{2}}$ is the

Hartmann number, $\text{Ec} = U_0^2 / [c_p (T_0 - T_\infty)]$ is the

Eckert number, $\lambda = QL^2 / (\mu c_p \text{Re})$ is the

dimensionless heat generation/absorption parameter,

$\text{Gr}_1 = g \beta (T_0 - T_\infty) L^3 / \nu^2$ is the Grashof number,

$\text{Re} = U_0 L / \nu$ is the Reynolds number,

$\text{Gr} = \text{Gr}_1 / \text{Re}^2$ is the thermal buoyancy parameter,

$\text{Pr} = \nu / \alpha$ is the Prandtl number, $N_1 = L^2 / (k \text{Re})$ is

the porous parameter, and $N_2 = 2C_b L / \sqrt{k}$ is the

inertia coefficient. In the above system of local

similarity equations, the effect of the magnetic field is

included as a ratio of the Hartman number to the

Reynolds number.

The physical quantities of interest in the problem are

the local skin friction acting on the surface in contact with the ambient fluid of constant density, which is defined as follows:

$$\tau_{wx} = \rho \nu \left(\frac{\partial u}{\partial y} \right)_{y=0} = \left(\frac{\rho \nu U_0}{L} \right) \left(\frac{\text{Re}}{2} \right)^{\frac{1}{2}} e^{\frac{x}{2}} f''(0) \quad \text{"(16)}$$

and the non-dimensional skin friction coefficient, C_f , can be written as

$$C_f = \frac{2\tau_{wx}}{\rho U_w^2} \text{ or } C_f \sqrt{\text{Re}_x} = \sqrt{2X} f''(0). \quad \text{"(17)}$$

The local surface heat flux through the wall with k as the thermal conductivity of the fluid is given by

$$q_{wx} = -k \left(\frac{\partial T}{\partial y} \right)_{y=0} = \frac{k(T_0 - T_\infty)}{L} \left(\frac{\text{Re}}{2} \right)^{\frac{1}{2}} e^{\frac{\alpha x}{2}} \theta'(0). \quad \text{"(18)}$$

(18)

The local Nusselt number, Nu_x , is defined as

$$\text{Nu}_x = \frac{x q_{wx}(x)}{k(T_w - T_\infty)}, \quad \text{"(19)}$$

$$\text{Nu}_x / \sqrt{\text{Re}_x} = -(X/2)^{\frac{1}{2}} \theta'(0), \quad \text{"(20)}$$

where Re_x is the local Reynolds number based on the surface velocity and is given by

$$\text{Re}_x = \frac{x U_w(x)}{\nu}. \quad \text{"(21)}$$

3. Numerical Solution: The system of transformed equations (13) and (14) together with the boundary conditions, have been solved numerically using the Keller box scheme, an efficient and accurate finite-difference scheme, as has been described in Cebeci and Bradshaw (1984). We first convert the second- and third-order differential equations, (13)-(14) into five first-order differential equations. Then we apply the finite difference scheme, which is described briefly as mentioned below.

The governing equations of the problem are given by

$$f''' + ff'' - (2 + N_2) f'^2 - 2 \left(\frac{\text{Ha}^2}{\text{Re}} + N_1 \right) e^{-x} f' + 2 \text{Gre}^{\alpha X/2} e^{-2X} \theta = 0 \quad \text{"(22)}$$

$$\text{Pr}^{-1}\theta + f\theta - \text{Gr}\theta + e^{X(2-a)/2} \text{Ec} \left(2 \frac{\text{Ha}^2}{\text{Re}} f^2 + f^2 e^{-X} \right) + 2\lambda e^{-X} \theta = 0 \tag{23}$$

$$f(0) = 0, f'(0) = 1, \theta(0) = 1 \text{ as } \eta \rightarrow 0 \tag{24}$$

$$f'(\infty) = 0, \theta(\infty) = 0 \text{ as } \eta \rightarrow \infty \tag{25}$$

In this method, the second-and third-order nonlinear differentialequations(13) and (14) have been reduced to five first order, ordinary differential equations as follows:

Let us define

$$f = f_0, \frac{df_0}{d\eta} = f_1 = f', \frac{df_1}{d\eta} = \frac{d^2 f_0}{d\eta^2} =$$

$$f_2 = f'', \frac{df_2}{d\eta} = \frac{d^3 f_0}{d\eta^3} = f_3 = f''',$$

$$\theta = \theta_0, \frac{d\theta_0}{d\eta} = \theta_1 = \theta', \frac{d\theta_1}{d\eta} = \frac{d^2 \theta_0}{d\eta^2} = \theta_2 = \theta''$$

(26)

Then we have

$$\frac{df_0}{d\eta} = f_1 \tag{27}$$

$$\frac{df_1}{d\eta} = f_2 \tag{28}$$

$$\frac{df_2}{d\eta} = -f_0 f_2 + (2 + N_2) f_1^2 +$$

$$2 \left(\frac{\text{Ha}^2}{\text{Re}} + N_1 \right) e^{-X} f_1 - 2 \text{Gr} e^{\alpha X/2} e^{-2X} \theta_0$$

$$\frac{d\theta_0}{d\eta} = \theta_1 \tag{30}$$

$$\frac{d\theta_1}{d\eta} = \text{Pr} \left[\begin{aligned} & -f_0 \theta_1 + a f_1 \theta_0 - e^{X(2-a)/2} \text{Ec} \\ & \left(2 \frac{\text{Ha}^2}{\text{Re}} f_1^2 + f_2^2 e^X \right) - 2\lambda e^{-X} \theta_0 \end{aligned} \right] \tag{31}$$

$$f_0(0) = 0, f_1(0) = 1, \theta_0(0) = 1, \tag{32}$$

$$f_1(\infty) = 0, \theta_0(\infty) = 0$$

Then applying finite difference scheme

Results and Discussion: A comparison of results for $\text{Ha}=\text{Gr}=\text{Ec}=\lambda=0$, as obtained by(i) Magyari and Keller (1999); (ii) Al-Odat et al.(2006); (iii) Pal and Mondal (2012); and (iv) the present method, is shown in Table 1. It is noticed that the present results are in close agreement with the published ones.

Fig. 2 shows the effect of the magnetic field parameter Ha^2 / Re on the horizontal velocity profile f' . The increasing frictional drag due to the

fact that applied transverse magnetic field produces a drag in the form of Lorentz force which results in decreasing the magnitude of velocity and thereby increase the temperature in the thermal boundary layer, which is the main cause for increasing the thermal boundary layer thickness.

Fig. 3 shows the variation of dimensionless horizontal velocity profile f' for various values of a . From this figure, it is observed that as the value of a increases there is increase in the value of the dimensionless horizontal velocity profile. The maximum dimensionless horizontal velocity profile is observed when $a = 7$.

Fig. 4 depicts the variation of dimensionless horizontal velocity profile for different values of dimensionless coordinate X . From this figure, it is noticed that dimensionless horizontal velocity profile decreases with increase in the values of X in the boundary layer, but the significant effect is noticed for flow adjacent to the stretching sheet.

Fig. 5 depicts the dimensionless temperature field for various values of a , with fixed values of other involved parameters. It is observed from this figure that temperature decreases with increase in the values of a . Further, it can be seen that the thermal boundary layer thickness decreases with increase in a . An interesting feature of this figure is that the heat transfer decreases throughout the boundary layer for positive values of a , which indicates that, the flow of heat transfer is directed from the wall to the ambient fluid whereas the rate of heat transfer in the boundary layer increases near the wall and decreases monotonically for negative values of a . The presence of temperature overshoot for negative values of a indicates that the maximum value of temperature occurs in the ambient fluid close to the surface but not over the surface.

Fig. 6 depicts the temperature profile in the fluid for various values of Ha^2 / Re , for $a = -2$ and $\text{Gr} = 0, 0.5$. It is noticed that an increase in the strength of magnetic field i.e., Lorentz force leads to an increase in the temperature far away from the wall, within the thermal boundary layer but the effect of magnetic field near the wall is to decrease the temperature in the absence of Grashof number. It is also noticed that the magnetic field enhances the thermal boundary layer thickness.

Effects of Grashof number on temperature profile for the values of $a = -2$ at $X = 0.5$ are depicted in Fig. 7, and it is noticed that increase in Grashof number leads to increase in temperature upto a certain value of η , and suddenly decreases and decays asymptotically to zero. Further, it is observed that this increase in temperature is due to the temperature difference between stretched wall and

the surrounding fluid. Increase in Gr leads to decrease in the boundary layer thickness.

Fig. 8 depicts the temperature profile $\theta(\eta)$ for various values of X along η for different values of $a = -1, -2$ and also Grashof number $Gr = 1.0$. It is noticed that the effect of increasing X on $\theta(\eta)$ is more effective for $a = -2$ than compared to the results obtained in the case when $a = -1$. It is interesting to note the behaviour of X on $\theta(\eta)$ is that the temperature overshoots near the wall for small value of X , for $a = -2$, whereas the overshoot diminishes when a is enhanced to $a = -1$ for all other values of X . It is also observed that the boundary layer thickness decreases with an increase in X .

Fig. 9 depicts the variation of temperature profiles $\theta(\eta)$ for various values of magnetic field parameter ($Ha^2 / Re = 0, 6, 8$) for two values of X . It is noticed that temperature decreases as X increases for all other fixed values of other involved parameters except when the value of parameter $a = 5$. It is also noticed that the thermal boundary layer thickness increases as X decreases and the effect of magnetic field is to increase the temperature for both values of X . This is due to the fact that magnetic field produces a Lorentz force which results in retarding force on the velocity, resulting in, increase in the temperature.

Fig. 10 depicts the effect of the Prandtl number Pr on dimensionless heat transfer parameter θ . It is noticed from this figure that as Prandtl number Pr increases, θ decreases. In heat transfer problems, the Prandtl number Pr controls the relative thickening of thermal boundary layers. When the Prandtl number Pr is

small, heat diffuses quickly compared to the velocity (momentum), especially for liquid metals, (low Prandtl number) the thickness of the thermal boundary layer is much bigger than the momentum boundary layer. Fluids with lower Prandtl number have higher thermal conductivities where heat can diffuse from the sheet faster than for higher Pr fluids. Hence the Prandtl number is a parameter that can be adjusted to increase the rate of cooling in conducting flows.

Fig. 11 depicts the effect of porous parameter N_1 over velocity profile, and it is

noticed from this figure that the velocity decreases with the increase of porous parameter, which offers resistance to the flow resulting in decrease of velocity in the boundary layer, which concurs with the results of various authors, whose works are concerned with porous medium, for instance the results of Pal and Mondal (2012).

Fig. 12 illustrates the effect of drag (inertia) coefficient of porous medium N_2 in the momentum boundary layer. From this figure it is noticed that the effect of drag coefficient is to decrease the velocity profile in the momentum boundary layer, which implies thinning of the boundary layer thickness.

Fig. 13 depicts the effect of heat source/sink parameter λ . It is observed that the boundary layer generates the energy, which causes the temperature profiles to increase, with increasing values of $\lambda > 0$ (heat source) whereas in the case of $\lambda < 0$ (absorption) boundary layer absorbs energy resulting in the temperature to fall considerably with decreasing in the value of $\lambda < 0$.

a		Pr					
		0.5	1	3	5	8	10
-1.5	(i)	0.20405	0.37741	0.92386	1.35324	1.88850	2.20000
	(ii)	0.19191	0.36152	0.90309	1.34143	1.82858	2.13693
	(iii)	0.20405	0.37741	0.92386	1.35324	1.88849	2.20003
	(iv)	0.192041	0.375270	0.924339	1.365939	1.940330	2.291212
-0.5	(i)	-0.17582	-0.29988	-0.63411	-0.87043	-1.15032	-1.30861
	(ii)	-0.18187	-0.32697	-0.67215	-0.84156	-1.08391	-1.25074
	(iii)	-0.17582	-0.29988	-0.63411	-0.87043	-1.15032	-1.30861
	(iv)	-0.180900	-0.299868	-0.642121	-0.895765	-1.215944	-1.40990
0.0	(i)	-0.33049	-0.54964	-1.12219	-1.52124	-1.99185	-2.25743
	(ii)	-0.31006	0.53104	-1.08522	-1.47558	-1.92666	-2.18847
	(iii)	-0.33049	-0.54964	-1.12219	-1.52124	-1.99184	-2.25742
	(iv)	-0.333726	-0.549499	-1.135373	-1.49179	-2.101447	-2.425285
1.0	(i)	-0.59434	-0.95478	-1.86908	-2.50014	-3.24213	-3.66038
	(ii)	-0.91903	-0.57771	-1.81039	-2.28864	-3.00587	-3.18620
	(iii)	-0.59434	-0.95478	-1.86907	-2.50013	-3.24212	-3.66037
	(iv)	-0.594841	-0.952890	-1.881801	-2.551345	-3.388378	-3.890687
3.0	(i)	-1.00841	-1.56029	-2.93854	-3.88656	-5.00047	-5.62820
	(ii)	-0.97665	-1.46569	-2.89007	-3.78072	-4.86245	-5.58576
	(iii)	-1.00841	-1.56030	-2.93854	-3.88656	-5.0046	-5.62820
	(iv)	-1.003639	-1.548572	-2.921988	-3.900769	-5.116296	-5.842330

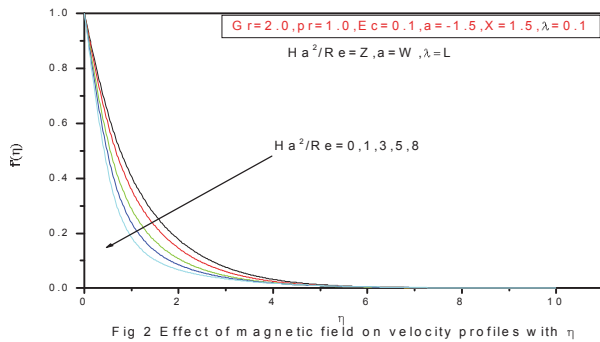


Fig 2 Effect of magnetic field on velocity profiles with η

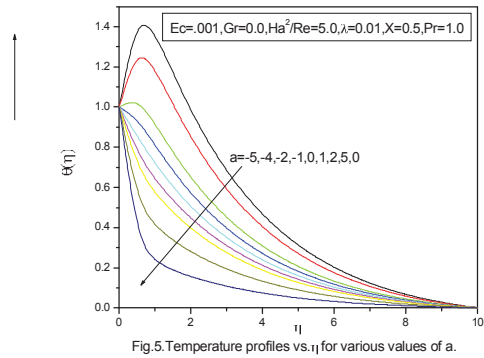


Fig.5. Temperature profiles vs. η for various values of a .

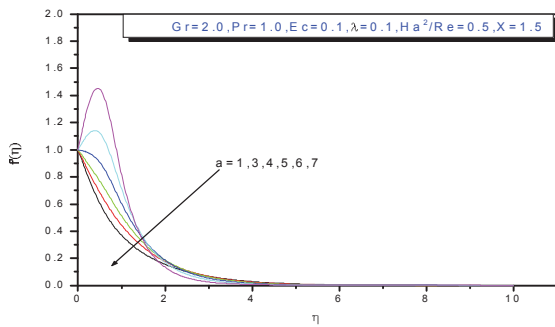


Fig.3. Variation of velocity profiles with η for various values of a .

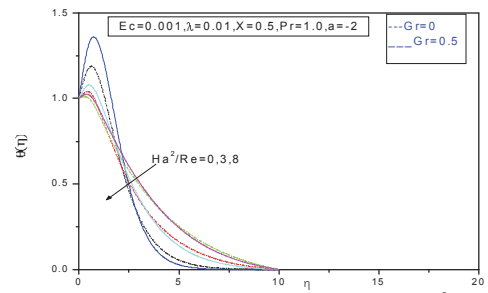


Fig.6. Temperature profiles vs. η for various values of Ha^2/Re and Gr .

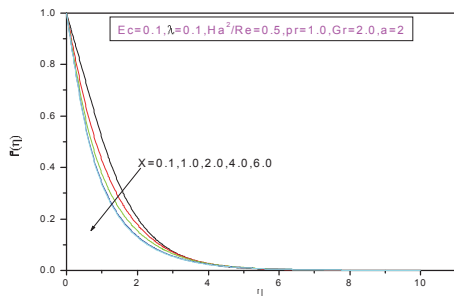


Fig.4. Variations of velocity profiles with η for different values of X .

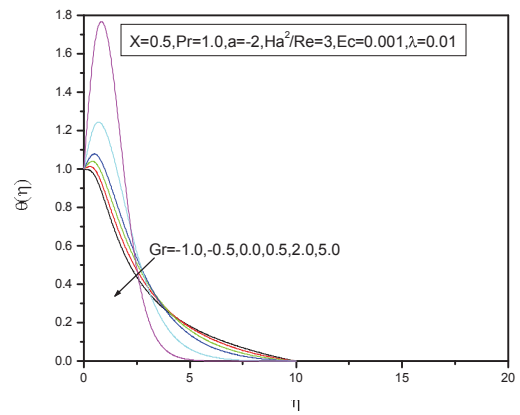


Fig7 temperature profile for various values of Gr

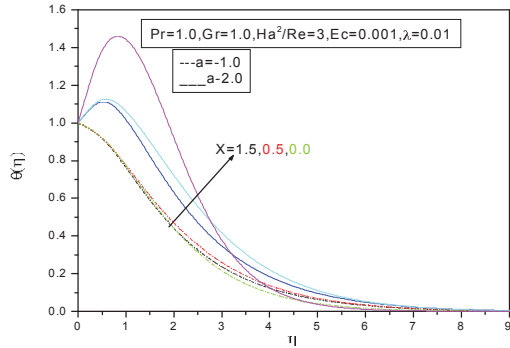


Fig.8. Temperature profiles vs. η for various values of a and X .

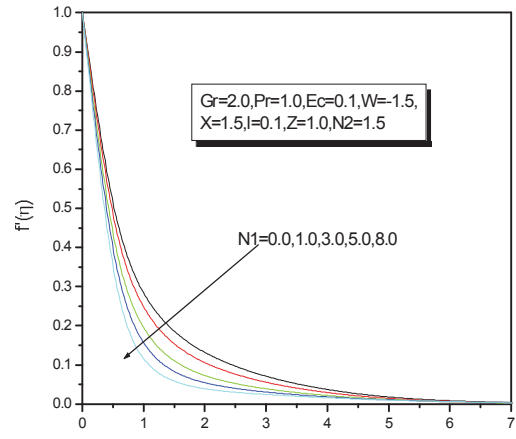


Fig.11. Temperature profile vs. η for various values of N_1 .

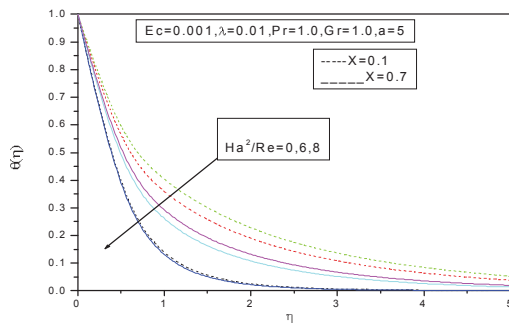


Fig.9. Temperature profiles vs. η for various values of Ha^2/Re and X when $a=5$.

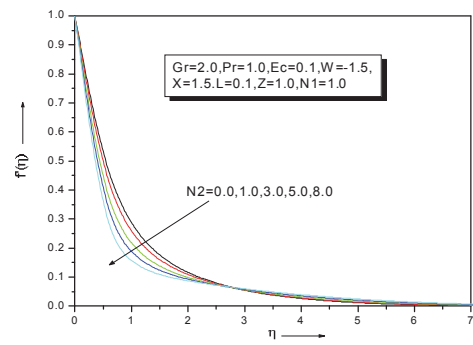


Fig.12. Temperature profile vs. η various values of N_2 .

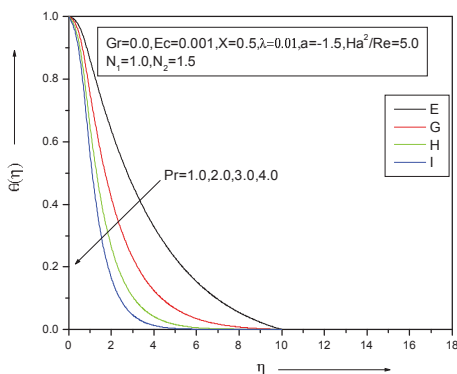


Fig10. Variation of temperature with η for different values of Pr

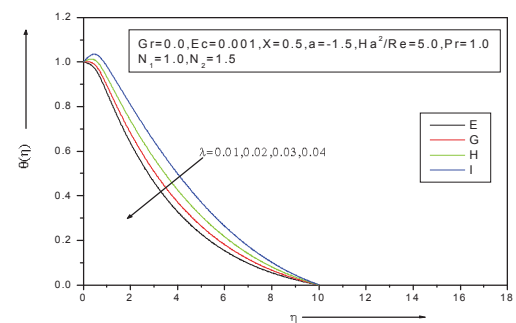


Fig13 Variation of temperature with η for different values of λ

A numerical method has been employed to study MHD boundary-layer flow and heat transfer due to a stretching sheet in the presence of a heat source/sink. The effects of the various governing parameters on the heat transfer characteristics have been examined.

The key observations can be summarized as follows.

1. The thickness of velocity boundary layer will decrease with an increase in the temperature distribution and magnetic parameters.
2. The temperature decreases with an increase in the value of the temperature distribution parameter, magnetic parameter, heat source or sink parameter, and the Prandtl number.
3. The thickness of the thermal boundary layer diminishes, with increase in both the temperature

distribution and Prandtl number parameters, and opposite result is observed for the magnetic parameter.

4. An increase in the temperature distribution parameter will increase both the skin friction coefficients and local Nusslet number.
5. An increase in the magnetic parameter will increase the skin friction.

Acknowledgment: This work is supported by UGC, Research Fellowship in Science for Meritorious Students (RFSMS) [void UGC Ltr. No.F.No. 7-72/2007(BSR) date 10.01.2012].

Ms. Veena.M. Basangouda author, acknowledges UGC for awarding the Research Fellowship.

References:

1. M.S. Abel, N. Mahesha, "Heat transfer in MHD viscoelastic fluid flow over a stretching sheet with variable thermal conductivity, non-uniform heat source and radiation", *Appl. Math. Model.* Vol.32, 2008, pp. 1965-1983.
2. E.M. Abo-Eldahab, "Convective heat transfer, by the presence of radiation, in an electrically conducting fluid at a stretching surface", *Can. J. Phys.* Vol. 79, 2001, pp.929-937.
3. A.A. Afify, "Similarity solution in MHD: Effects of thermal diffusion and diffusion thermo on free convective heat and mass transfer over a stretching surface considering suction or injection. *Commun*", *Nonlinear Sci. Num. Simul.* Vol.14, 2009, pp.2202-2214.
4. M.E. Ali, "On thermal boundary layer on a power-law stretched surface with suction or injection", *Int. J. Heat Fluid Flow.* Vol.16, 1995, pp.280-290.
5. M.Q. Al-Odat, "Damseh, R.A., Al-Azab, T.A.: Thermal boundary layer on an exponentially stretching continuous surface in the presence of magnetic field effect", *Int. J. Appl. Mech. Eng.* Vol. 11, 2006, pp.289-299.
6. H.I. Andersson, K.H. Bech, "Magnetohydrodynamic flow of a power-law fluid over a stretching sheet", *Int. J. Non-Linear Mech.* Vol.27, 1992, pp.929-936.
7. A. Bejan, K.R. Khair, "Heat and mass transfer by natural convection in porous medium", *Int. J. Heat Mass Transf.* Vol.28, 1985, pp.909-918.
8. T. Cebeci, P. Bradshaw, "Physical and Computational Aspects of Convective Heat Transfer", Springer-Verlag, New York, 1984.
9. E.M.A. Elbasha, "Heat transfer over an exponentially stretching continuous surface with suction", *Arch. Mech.* Vol. 53, 2001, pp.643-651.
10. P. Forchheimer, *Z. Wasserbewegung durc Bode n, Ver. Deutsch Ing.* Vol.45, 1901, pp.1782-1788.
11. P.S. Gupta, A.S. Gupta, "Heat and mass transfer on stretching sheet with suction or blowing", *Can. J. Chem. Eng.* Vol.55, 1977, pp.744-746.
12. S.K. Khan, E. Sanjayanand, "Viscoelastic boundary layer flow and heat transfer over an exponential stretching sheet", *Int. J. Heat Mass Transf.* Vol.48, 2005, pp.1534-1542.
13. V. Kumaran, G. Ramanaiah, "A note on the flow over a stretching sheet". *Acta Mech.* Vol.116, 199, pp.229-233.
14. E. Magyari, B. Keller, "Heat and mass transfer in the boundary layers on an exponentially stretching continuous surface" *J. Phys. D: Appl. Phys.* Vol.32, 1999, pp.577-585.
15. D. Pal, "Heat and mass transfer in stagnation-point flow towards a stretching surface in the presence of buoyancy force and thermal radiation", *Meccanica* Vol.44, 2009, pp.145-158.
16. D. Pal, "Mixed convection heat transfer in the boundary layers on an exponentially stretching surface with magnetic field". *App. Math. Comp.* Vol. 217, 2010, pp.2356-2369.
17. D. Pal, S. Chatterjee, "Heat and mass transfer in MHD non-Darcian flow of a micropolar fluid over a stretching sheet embedded in a porous media with non-uniform heat source and thermal radiation. *Commun*", *Nonlinear Sci. Num. Simul.* Vol.15, 2010, pp.1843-1857.
18. D. Pal, H. Mondal, "Soret and Dufour effects on MHD non-Darcian mixed convection heat and mass transfer over a stretching sheet with non-uniform heat source/sink", *Physica B: Condensed*

Matter Vol. 407,2012,pp.642-651.

19. K.B.Pavlov, "Magnetohydrodynamic flow of an incompressible viscous fluid due to deformation of a plane surface. Magnetohydrodyn". Vol. 10,1974,pp. 507-510.

20. O.A.Plumb,J.C.Huenefeld, "Non-Darcy natural convection from heated surfaces in saturated porous media".Int. J. Heat MassTransf.Vol.24,1981,pp.765-768.

Professor, Research scholar
Department of Mathematics, Gulbarga University,
Gulbarga-585106, Karnataka, India